A review of DC/DC converter-based electrochemical impedance spectroscopy for fuel cell electric vehicles

Hanqing Wang, Arnaud Gaillard, Daniel Hissel

A review of DC/DC converter-based electrochemical impedance spectroscopy for fuel cell electric vehicles

Hanqing WANG [a, c, *], Arnaud GAILLARD [a, c], Daniel HISSEL [b, c]

[a] FEMTO-ST, CNRS, Univ. Bourgogne Franche-Comte, UTBM

[b] FEMTO-ST, CNRS, Univ. Bourgogne Franche-Comte

[c] FCLAB, CNRS, Univ. Bourgogne Franche-Comte

[*] Corresponding author: hanqing.wang@utbm.fr

Abstract-- Considering transport applications, there is worldwide an increasing interest in the use of hydrogen-energy for supplying electric powertrains. In order to extend the fuel cell lifespan and to increase its reliability and efficiency, the following features are essential to a fuel cell stack connected DC/DC boost converter: low input current ripple, high voltage gain ratio, high efficiency, high compactness, and high redundancy. Moreover, in order to assess in real time the state-of-health of the fuel cell stack, on-line Electrochemical Impedance Spectroscopy (EIS) functionality integrated with the fuel cell stack connected DC/DC boost converter is a real promising solution requiring no additional measurement equipment. From these points of view, this paper presents a comparison analysis of high voltage gain DC/DC boost converters for fuel cell electric vehicles applications. In addition, some comments and guidelines regarding integration issues are also provided.

Keywords-- On-line EIS, PEMFC, Fault Detection, DC/DC converter, FCEV

I. Introduction

During the last decade, transportation-related air pollution emissions have reached increased consideration from the political, technical and scientific communities. In the general trend towards decreasing crude oil dependence, hydrogen-energy based technologies and fuel cell systems are more and more treated as indispensable parts in the upcoming next-generation environmentally friendly vehicle [1]. Indeed, they are enhancing performances and lowering fabrication costs; owing to the actual duality between hydrogen-energy and electricity, fuel cell electric vehicles (FCEV) present the advantages of a high efficiency and a (in-situ) zero pollutant emission relative to classical internal combustion engine vehicle. Moreover, their refueling time is quite similar to that of conventional oil-fueled automotive. Proton Exchange Membrane Fuel Cell (PEMFC), which owns the advantages such as low operating temperature, quick start-up and rapid load following, is seen as the most suitable type of fuel cell for transportation applications.

Nevertheless, before the mass marketization of FCEV, there are still technical and scientific issues to be solved. The most urgent subject is the limited lifespan of the existing PEMFC systems, especially when considering hard operating constraints. Depending on recent publications from the U.S. department of energy, the maximum life expectancy of an existing fuel cell system under transportation operating conditions is around 3000 hours; however, at least 5000 hours are demanded to reach the “standard” lifetime of internal combustion engines [2]. In order to achieve this purpose, not only studies on materials, bipolar plates, catalytic layers, and electrolytic membranes must be in progress, but also research towards extending the lifespan and increasing the reliability must be done from the overall perspective. Hence, diagnostic approaches and state-of-health management strategies are essential to be developed to increase the durability, the efficiency and the reliability of the fuel cell stack and the fuel cell system obviously [3]. Furthermore, in order to increase the dynamic performances of the fuel cell system, the mixed use of the fuel cell stack and auxiliary power sources such as electrochemical or electrostatic electricity storage devices must be considered [3].

Taking into consideration of PEMFC’s inherent characteristic (low voltage and high current) and voltage requirement of motor drive system, power converter is essential to be connected between PEMFC and the motor drive system in order to realize power conditioning. Generally, power converters can be classified as non-isolated converters and isolated converters. The former achieves a simple structure and high compactness, but voltage gain ratio is relatively low; the latter can obtain high voltage ratio, however, intermediate AC stage, which is composed of transformer and inverter, will reduce the compactness. Magnetic components based on coupled structure are attractive to reduce volume and weight and to gain compactness and space for the fuel cell system. To be emphasized, depending on the study of [4], the fuel cell current ripple can influence the fuel cell lifespan. In other words, a power converter which can reduce the input

current ripple and the volume and weight will be more suitable for FCEV application. Nowadays, Wide-Band Gap (WBG) semiconductors have been commercialized and applied in actual FCEV [5]. This new generation semiconductor is much suitable for high power and high switching frequency applications; and better thermal performance, lower power losses, and higher compactness will be reached. Thus, the reliability, energy efficiency and power density of the fuel cell system will also be enhanced.

Electrochemical impedance spectroscopy (EIS) is established as a powerful characterization tool to detect different failure mechanisms occurring in the fuel cell [6]. As fuel cell systems should be able to enter the market at competitive prices, hence, the use of a minimal number of actual sensors is demanded. Besides, this requirement will also reduce complexity within the system and increase reliability. Thus, the integration between EIS and control strategy of the necessary power converter provides the possibility to realize on-line diagnosis of the fuel cell stack without any additional sensor or equipment [7].

This paper is organized as follow. Section II will provide some recalls about fuel cell technology and fuel cell systems. The fuel cell electric vehicle's development will be compared in details. Then, section III will be devoted to the power converter development for FCEV application. The approaches to increase voltage gain ratio and the development of WBG semiconductors are separately commented. In section IV, online EIS detection process of PEMFC integrated with power converter is mainly discussed. Relevant studies are summarized; the advantages and disadvantages of each method are demonstrated. Finally, this paper will be concluded in section V. A general suggestion will be proposed to achieve a proper power converter for FCEV application, which can not only realize power conversion with high performances, but also accomplish online diagnosis of the fuel cell stack without any additional equipment.

II. Fuel cell electric vehicle development

Nowadays, researchers of the automotive field devote themselves to developing economic and environment-friendly vehicles. Among these clean energy based vehicles, all-electric vehicles (EVs), plug-in hybrid electric vehicles (PHEVs), hybrid electric vehicles (HEVs) and fuel cell electric vehicles (FCEVs) are playing dominant roles. The researches of EVs, PHEVs and HEVs have been started early, the technologies are more mature, and have already realized large-scale marketization.

EVs are propelled by one of more electric motors powered by a rechargeable battery and achieve several performance benefits such as quiet operation, quick acceleration ability, regenerative braking, and less requirement of maintenance than internal combustion engines. PHEVs are hybrids that can be charged both by plugging them into an electrical outlet or charging station. Both PHEVs and HEVs are classified by two configurations: series PHEVs/HEVs which are also called Extended Range Electric Vehicles (EREVs), and parallel or blended PHEVs/HEVs. The electric motor of series PHEVs/HEVs is the only power source that turns the wheels; the gasoline engine only generates electricity. For the parallel PHEVs/HEVs, both the engine and electric motor are mechanically connected to the wheels, and both may propel the vehicle. HEVs combine the best features of the internal combustion engine with an electric motor and can significantly improve fuel economy. They are primarily propelled by an internal combustion engine; they also use regenerative braking to convert energy normally wasted during coasting and braking into electricity [8].

However, EVs, PHEVs and HEVs have several disadvantages. Firstly, the charging times of EVs and PHEVs still requires several hours (except fast charging phases). Secondly, the driving ranges of EVs are still quite limited; moreover, it is more sensitive to driving style, driving conditions, and accessory use. Thirdly, PHEVs and HEVs still rely on the crude oil which means cannot realize real "zero" pollutant emission. Briefly, FCEVs have many advantages (fast refueling, long driving range, zero pollutant emission, etc.) over the other types of clean energy vehicles. Different fuel cell electric vehicles and fuel cell technologies are firstly discussed blow.

Since the occurrence of first modern fuel cell electric vehicle around 1959 [9], many car manufacturers have focused on the study of FCEV. In 2000, Ford Motor Company has presented a two-wheel drive compact car which was powered by a fuel cell stack and electrochemical batteries. In 2005, a four-wheel drive model of a fuel cell vehicle has been rolled out by Ford and the driving range was 200 miles. Mercedes-Benz has also rolled out two models of its FCEV, the F-Cell, separately in 2002 and 2010. The power level and driving range of the former were 65kW and 100 miles, while 100kW and 190 miles have been achieved by the latter [10].

In today's market, commercial fuel cell electric vehicles proposed by Toyota Motor Corporation, Honda Motor Company, and Hyundai Motor Company have taken the major part of the market. A global comparison analysis of the commercialized FCEV from these three companies has been presented in Table. I. According to this table, obviously PEM fuel cell is the common choice of these companies.

Table. I. Overall comparison analysis of the commercialized FCEV [10]

	Toyota FCHV-adv	**Toyota Mirai**	**Honda FCX-Clarity**	**Honda Clarity Fuel Cell**	**Hyundai Tucson ix35 FCEV**	**Hyundai Nexo**

Year		2008	2015	2008	2016	2014	2018
Vehicle class		Sport Utility Vehicle 2WD	Subcompact car	Midsize car	Midsize car	Small Sport Utility Vehicle 2WD	Small Sport Utility Vehicle 2WD
Fuel cell	Type	PEM	PEM	PEM	PEM	PEM	PEM
	Cell quantity	400 cells (dual line stacking)	370 cells [11] (single line stacking)	--	--	434 cells (250~450V)	440 cells [17] (255~450V)
	Power density	1.4kW/L 0.83kW/kg	3.1kW/L [12] 2.0kW/kg	2.0kW/L 1.0kW/kg	3.1kW/L [14] 2.0kW/kg	1.65kW/L [16]	3.1kW/L [17]
Fuel	Type	Hydrogen	Hydrogen	Hydrogen	Hydrogen	Hydrogen	Hydrogen
	Storage pressure (nominal)	--	70MPa	35MPa	70MPa	70MPa	70MPa
	Storage volume	156L	122.4L	171L	141L	144L	156.6L
	Fuel storage mass	--	5.0kg	3.6kg	5.0kg	5.64kg	6.33kg
	Refueling time	--	3 minutes	--	3 minutes	3 minutes	3 minutes
DC/DC converter for fuel cell		No	Yes [13]	No	Yes [14]	No	No [17]
DC bus voltage		--	650V [13]	330V	500V [14]	400V	400V [17]
HV battery	Type	Ni-MH	Ni-MH	Li-Ion	Li-Ion	Li-Ion	Li-Ion
	Voltage	288V	245V	288V	358V	180V	240V
Motor	Type	AC Synchronous Motor	AC Synchronous Motor	DC Brushless Motor	PMSM	AC Induction Motor	PMSM
	Power	90kW-260Nm	113kW	100kW	130kW	100kW	120kW
Driving range (miles)		--	312	240	366	265	354
Fuel economy: Miles per Kilogram (city/highway)		--/--	66/66	60/60	68/66	48/50	58/53

For the new generation FCEVs of Toyota Motor Corporation and Honda Motor Company, the fuel cell power densities have been increased compared with previous models. The PEMFC of Toyota Mirai has been redesigned and resulted in lower concentration overvoltage, lower resistance overvoltage and lower activation overvoltage. Then, the Mirai stack increased the current density by a factor of 2.4 compared to the stack of Toyota FCHV-adv, and the cell volume has been reduced by 24%. As a result, the FC system of Toyota Mirai increased the power density by more than twice that of the conventional stack [12]. The new generation FCEV of Honda Motor Company, Honda Clarity Fuel Cell, employed Honda's unique 2-cell cooling structure. As a result, new cell thickness has been reduced by 20% compared with previous cell, and electricity generation for each cell has been improved by 1.5 times which allows the decrease of the number of cells by 30%. Thus, the Clarity fuel cell system also increased the power density. However, the thinner gas flow path require a higher pressure operating point than before [14]. Considering the hydrogen storage system, higher storage pressure is preferred to reduce storage volume and gaining inner space. The powertrain structures of these commercialized FCEV are presented in Fig. 1. In Fig. 1.(a), PEMFC is connected to DC bus directly without power converter. This structure has been selected by Toyota FCHV-adv (2008), Honda FCX-Clarity (2008), Hyundai Tucson ix35 FCEV (2014) and Hyundai Nexo (2018). The power control unit of this structure is simple. However, the output voltage of a single cell is quite low (<1V) and the voltage requirement of the motor drive system is high (at least 330V according to Table. I), which means whether quantities of single cells are requested to be connected in series or multi-stack structure is requested. This leads to air, hydrogen, cooling water issues in the stack or increased control complexity. At the same time, the power density of fuel cell system can be decreased. The new generation FCEV, Toyota Mirai and Honda Clarity Fuel Cell, have changed their powertrain structure to Fig. 1 (b). The improvement is that a DC/DC converter is connected between PEMFC stack and DC bus. The output voltage of the PEMFC stack will be boosted to higher level. Meanwhile, according to Table. I, when the motor's maximum drive voltage is increased, the motor's maximum output and maximum torque will also be increased.

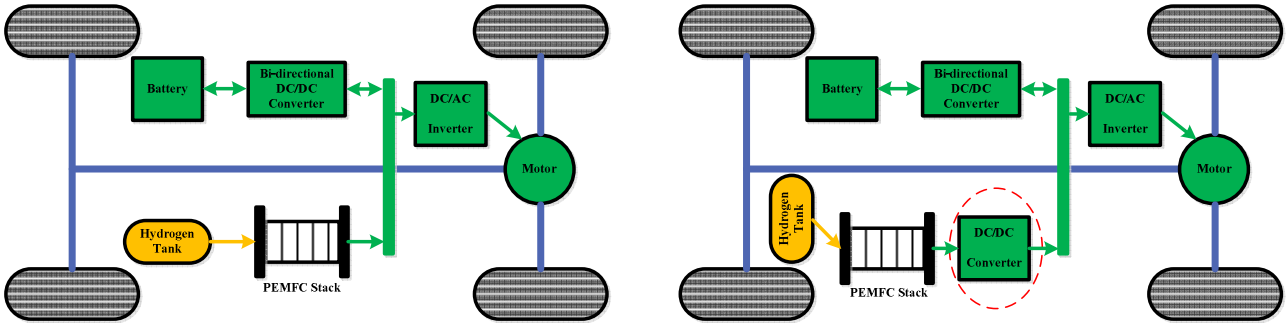

(a) Uncontrolled FC combined with controlled Battery (b) Controlled FC combined with controlled Battery

Fig. 1. The powertrain structures of the commercialized FCEV

III. DC/DC converter for FCEV application

As discussed in the previous section, using power converter as an interface between the fuel cell system and DC bus shows great advantages such as increasing motor output level and enhancing PEMFC power density and reliability. DC/DC power converters are always classified as non-isolated DC/DC converters and isolated DC/DC converters [22] [23]. The schematic representation of these two kinds of power converters is shown by Fig. 2.

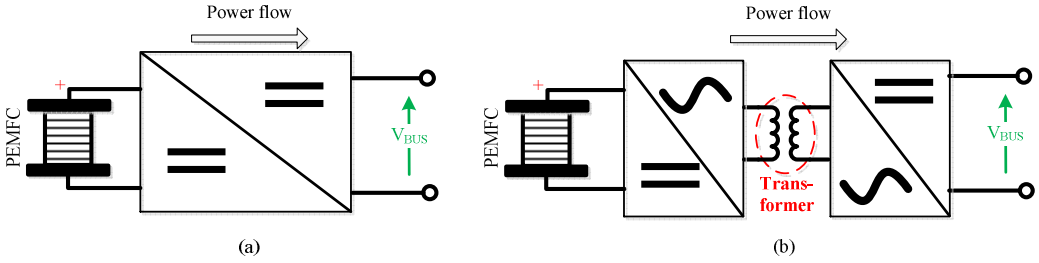

Fig. 2. Schematic representation of (a) Non-isolated DC/DC converters and (b) Isolated DC/DC converters

The non-isolated DC/DC converters are widely used due to their simple structure, high compactness, low cost and simplified control. Some non-isolated topologies as Boost converter, Buck-Boost converter, Cuk converter, and Sepic converter are well-known. Unlike the other three topologies, in whole duty cycle range (from zero to one), the voltage gain ratio of a Boost converter is always higher than one; and the output voltage is positive with respect to the input voltage [24] [25].

Due to the existence of a magnetic transformer, the isolated DC/DC converters are more suitable for the application that requests a high voltage gain ratio. Another characteristic of the isolated DC/DC converters is the galvanic isolation. However, magnetic transformer leads to poor compactness, higher weight and more complex design. The isolated power converters are a combination of two stages: the primary DC/AC stage (Half-bridge inverter, Full-bridge inverter, etc.) and the secondary AC/DC stage (controlled or uncontrolled rectifier). Other well-known isolated topologies are as: Push-pull converter, Forward converter, and Flyback converter.

Towards the FCEV application, the following criteria are essential to be satisfied to design or select a proper power conditioning unit:

- High efficiency, which is closely related to the fuel economy and the design process of the powertrain cooling system;
- High voltage gain ratio, which is required by the inherent characteristics of the FC stack;
- High compactness, low weight and volume are essential due to the limited inner space of the FCEV;
- Low input current ripple is requested to extend the FC stack's lifespan;
- Low cost and high reliability are mandatory to ensure commercialization.

Non-isolated DC/DC boost converters based on the interleaved structure are helpful to reduce the FC current ripple and the weight and size of the FC system [13]. Wide-Band Gap (WBG) semiconductors-based power switches have been commercialized and are a better choice than conventional Si semiconductors-based ones to improve thermal performance and efficiency of a power converter [14]. Power converters based on coupled magnetic components are possible to increase compactness, reduce weight and increase voltage gain [26]. Meanwhile, auxiliary circuits that focus on increasing voltage gain ratio are also attractive for FCEVs application [27]. Power converters for FCEVs applications, based on these technologies, will be analyzed in the following subsections.

3.1. Power converters based on the interleaved structure

Interleaved Boost Converter (IBC), as presented in Fig. 3 (a), has been developed focusing on reducing power source current ripple while retaining the same voltage gain ratio as the conventional Boost converter [28]. Benefiting from the specific structure, the input current is shared by multiple parallel power switches, hence, current stress of each power switch can be reduced and total efficiency of the converter can be increased. Concerning the real FCEVs applications, Wen et al. [29] have presented a 150kW, 2-phase hybrid-mode IBC. A 500W 3-phase IBC prototype based on Maximum Power Point Tracking (MPPT) controller has been analyzed by Benyahia et al. [30]. A 4-phase IBC has been adopted by Toyota Mirai [13] to increase the voltage of the motor and to reduce the number of fuel cell stack cells.

Floating Interleaved Boost Converter (FIBC), as presented in Fig. 3 (b), has also been widely studied for FCEVs application due to its ability that can not only reduce the power source current ripple but also increase the voltage gain ratio [31] [32]. However, the control design is more complex than for IBC.

According to a recent study, a novel 50kW prototype Floating Interleaved Buck-Boost Converter (FIB-BC) for fuel cell electric vehicle applications has been proposed by Gao et al. [33] and shown in Fig. 3 (c). The proposed topology provided significant mitigation of the boost module and buck module with switching between the step-up and step-down modes, lowering input current ripple and improving efficiency and reliability. High efficiencies have been achieved which were kept above 95%.

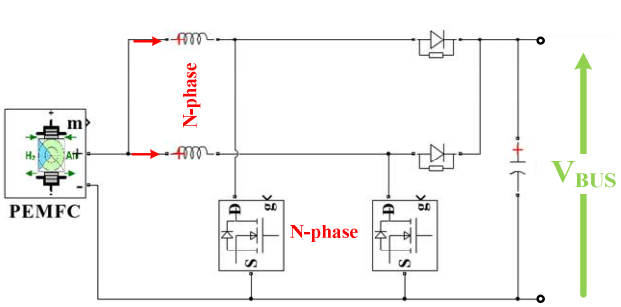

(a) N-phase IBC [29] [30]

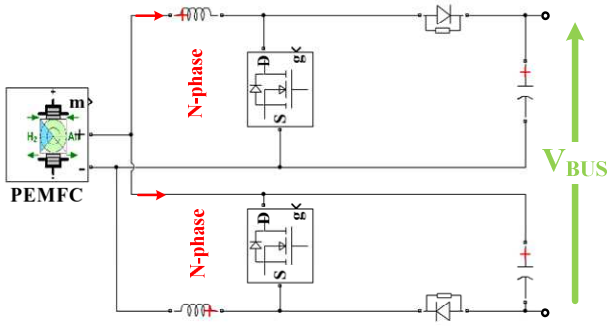

(b) N-phase FIBC [31] [32]

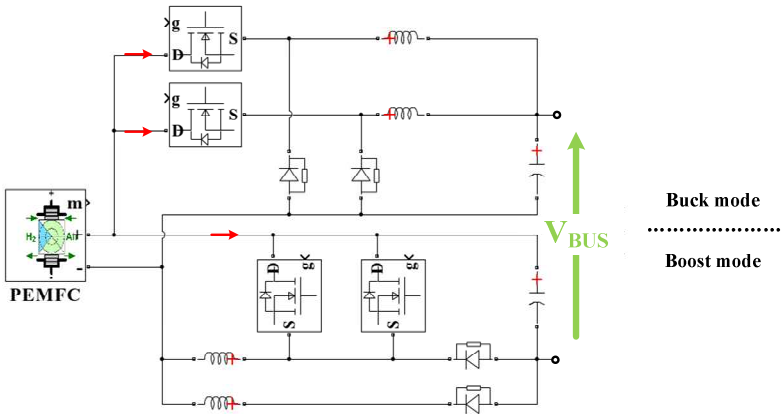

(c) 4-phase FIB-BC [33]

Fig. 3.Schematics of non-isolated DC/DC converters for FCEVs application based on the interleaved structures

3.2. Power converters based on WBG semiconductors

Nowadays, the new generation Wide Band-Gap (WBG) semiconductors that feature high power density, high efficiency, and good thermal performance are quite suitable for FCEV applications. Silicon Carbide (SiC) and Gallium Nitride (GaN) are the most promising candidates to replace Silicon (Si) in the next generation of power switches [34]. Fig. 4 presents the material properties of Si, SiC, and GaN [35]. The high critical field of both GaN and SiC is a property which allows these devices to operate at high voltages and low leakage currents. Higher electron mobility and electron saturation velocity allow for a higher frequency of operation. Higher thermal conductivity means that the material is superior in conducting heat efficiently. Higher thermal conductivity combined with wide bandgap and high critical field gives SiC semiconductors an advantage when high power is a key device feature.

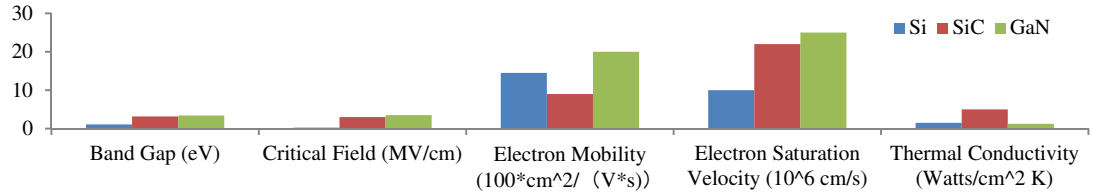

Fig. 4. The material properties of Si, SiC and GaN

According to [36], the SiC semiconductor-based power switches have been identified as a prime option for the FCEV applications, which is benefited by the characteristics of the specific material. Though the Si-IGBT are chosen for the high power design, the low switching frequency, relatively low maximum operating temperature, and high switching losses are the limits for the application in high frequency, high power fields. According to [14], SiC power module [15] has been used for the first time in a production vehicle, and the size of the FC voltage converter unit has been reduced.

Table. II presents the WBG semiconductors based power converters/inverters for transportation applications. Among these studies, some of them focused on the fuel cell powered more electric aircraft (MEA) application [37] [38] and military electric vehicle application [39], where the operating conditions are much extreme than the daily transportation applications. Meanwhile, in order to make a more comprehensive presentation of the WBG semiconductors applications, fuel cell connected DC/DC power converters [37] [38] [40], battery connected bi-directional DC/DC power converters [41] [39], and motor drive system's inverters [42] [43] are presented.

These power converters and inverters are all realized and verified by experiments. Obviously, high switching frequencies (50~200kHz) have been used by the SiC/GaN MOSFET based power converters and inverters. In some applications, only SiC semiconductors are used [41] [38]; in others, different types of semiconductors are used mixed. All of these topologies have very high efficiencies which are commonly over 98%. Benefiting from this advantage, better thermal performances have been achieved, and the requirements for the heat dissipation systems have been reduced. Hence, the compactness and the reliability of power conditioning units have been increased.

Table. II. Power converter/inverter based on WBG semiconductors for transportation applications

Topology	**Ref**	**Power level**	**Switching frequency**	**Max Efficiency**	**Semiconductor**			**Application field**
					Type	**Quantity**	**Part No.**	
Bi-directional DC/DC Half-Bridge converter	[41]	2kW	150kHz, 200kHz	98.8%	SiC MOSFET	2	1200V 24A CMF20120D (CREE)	EV; HEV; Plug-in EV; FCEV.
					SiC SBD	2	1200V 54A C4D40120D (CREE)	
6-phase IBC	[37]	15kW (6 parallel fuel cell)	--	~97%	SiC MOSFET	--	--	FC powered MEA
					No information of diodes.			
Bi-directional DC/DC Half-Bridge converter	[39]	100kW (continuous), 150kW (peak)	--	98% at 100 ambient temperature	Si IGBT	--	--	Military EV
					SiC diode	--	--	
Three-phase Half-Bridge inverter	[42]	30kW	20kHz	99%	SiC MOSFET power module	3	1200V 300A CAS300M12BM2 (CREE)	EV; HEV; Plug-in EV; FCEV.
					No information of diodes.			
Three-phase Half-Bridge inverter	[43]	30kW (continuous), 55kW (peak)	20kHz	98.9%	SiC MOSFET power module	3	1200V 444A CAS325M12HM2 (CREE)	EV; HEV; Plug-in EV; FCEV.
					Schottky barrier diode	6	--	
Floating-Output Interleaved-Input boost	[38]	60kW (2kV Vin)	50~100kHz	98.7%	SiC MOSFET	2	3.3 kV XPM3-3300-0040-ES (CREE)	FC powered MEA
					SiC schottky diode	2	CPW3-3300-Z045B (CREE)	
Three level boost	[40]	1.1kW & 1.3kW	100kHz	--	GaN MOSFET	2	GS66508T E-HEMTs (GaN Systems)	FCEV
					SiC schottky diode	3	C3D10065E (CREE)	

3.3. Power converters based on coupled magnetic components

As studied previously, power converters based on the interleaved structure are quite suitable for FCEVs application. However, the increase in the number of branches will lead to an increase in the quantity of magnetic components. Since the fuel cell connected power converter has to constantly pass the high power generated by the fuel cell, the inductors require high heat dissipation performance. For example, the 4-phase IBC of Toyota Mirai used liquid loop cooling (LLC) to improve the heat dissipation capacity by reducing the thermal resistance [13]. In contrast, the extra liquid coolant is required, and the global structural design of the power converter is much more complicated.

Magnetic components based on the coupled structure can contribute a lot to reduce size and weight, to decrease quantities, and to reduce power losses [44]. Thus, the coupled inductors can lead to less heat dissipation and the cooling system can be simplified accordingly. The number of interleaved branches, the method of coupling, and the shape of a magnetic core influence the performances of power converters strongly. Table. III presents the interleaved power converters based on different types of coupled inductors. In order to present a full comparison, the application fields are not limited to FCEVs; power conditioning units for EVs/HEVs/PHEVs applications are also studied.

Table. III. Interleaved power converters combined with coupled inductors for electric vehicles

Basic topology	Ref	Power level	Magnetic component				Efficiency	Application field
			Coupling method	Quantity	Shape	Material		
2-phase IBC	[45]	3.6kW 72kW	Inverse coupled; 2 windings for a single core.	1	CCTT	--	-- ~96.7%	FCEV
2-phase IBC	[46]	450W	Inverse coupled; 4 windings for a single core.	1	E-E (E42/21/15)	3C92	~96%	FCEV
2-phase IBC	[47]	1kW	Uncoupled	2	EE90	--	--	FCEV
			Loosely inverse coupled; 2 windings for a single core.	1	EE60	--	~98%	
			Integrated inverse coupled; 2 windings for a single core.	1	EE50	--	~97.61%	
2-phase IBC	[48]	1kW	Inverse coupled; 2 windings for a single core.	1	--	--	--	FCEV
2-phase IBC	[49]	1kW	Inverse coupled; 2 windings for a single core.	1	EC70	PC40	--	FCEV
2-phase IBC	[50]	500W	Direct coupled; 2 windings for a single core.	1	--	--	~95.5%	FCEV
3-phase IBC	[52]	545W	3 windings for each core	3	E-E	--	~97%	FCEV
2-phase IB-BC	[51]	360W	Inverse coupled; 2 windings for each core.	4	Toroid	--	--	FCEV
2-phase BIB/BC	[55]	--	Inverse coupled; 2 windings for a single core.	1	U-I	3F45	~98.5%	EV/HEV/PHEV/ FCEV
4-phase BIB/BC	[56]	120W (buck) 36W (boost)	Inverse coupled; 4 windings for a single core.	1	Customer design	DMR50B	~94.1% ~90.33%	EV/HEV/PHEV/ FCEV
Interleaved forward-flyback	[54]	2kW	Direct coupled; 3 windings for each core.	2	Toroid	--	~96.5%	FCEV

Obviously, N-phase IBCs are mostly used for FCEVs application. Both the inverse coupled structure [45] [47] [48] [49] and the direct coupled structure [50] have been integrated with this specific topology. H. Liu et al. [46] proposed a 2-phase inverse coupled IBC (IICIB) without right half-plane zeros. Besides, B.C. Barry et al. [51] and Tseng, K. C et al. [54] also separately proposed a 2-phase inverse coupled Interleaved Buck-Boost Converter (IB-BC) and a direct coupled Interleaved Forward-Flyback converter for FCEVs application. Towards EV/HEV/PHEV applications, a bi-directional buck/boost converter is essential as the interface between the energy storage system and the DC bus. Huang, X. et al. [55] and Yang, Y. et al. [56] have proposed a 2-phase and a 4-phase Bi-directional Interleaved Buck/Boost Converters (BIB/BCs), respectively.

According to the comparative studies, most of the topologies use the magnetic cores which are widely commercialized and easily to be obtained, for example, the E-E shaped cores and the toroid cores. Martinez, W. et al. [47] have made an overall comparative study of 2-phase IBC based on different coupling manners. According to this research, although the Integrated Winding Coupled Inductor (IWCI)

can reduce the size, it can lead to a magnetic loss increase. On the other hand, this research suggests that the Loosely Coupled Inductor (LCI) converter is effective for reducing the size and improving the efficiency.

When the number of interleaved phases is bigger than two, there are more coupling manners to be selected such as symmetrical cascade association [56], cyclic cascade association [52], symmetrical parallel association, and cyclic parallel association [53]. Concerning different methods, the number of magnetic cores and the complexity of coupling is quite different.

A 4-phase magnetic core with the monolithic structure is used for the proposed converter in [56]. Although the number of magnetic component has been reduced, the redundancy of the converter is decreased, and the manufacturing difficulty and cost of the specific-made magnetic core are increased which are unfavorable for commercialization. The structure of multi-magnetic cores has been selected in the study of [52] where a 3-phase IBC based on coupled inductors has been proposed. Each two neighbor branches are coupled by a single E-E magnetic core and then the three independent E-E magnetic cores are coupled based on the cyclic cascade association. Hence, the redundancy of the proposed converter in [52] is higher than the one of [56]. The topologies which are mentioned in Table. III are presented in Fig. 5.

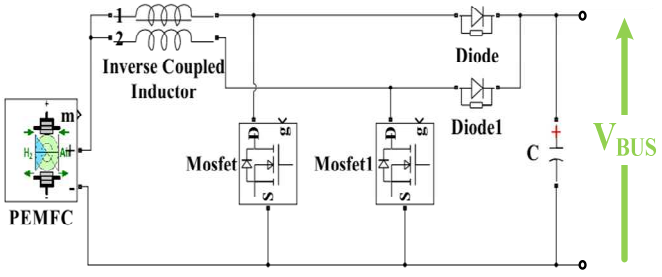

(a) 2-phase inverse coupled IBC by [45] [47] [48] [49]

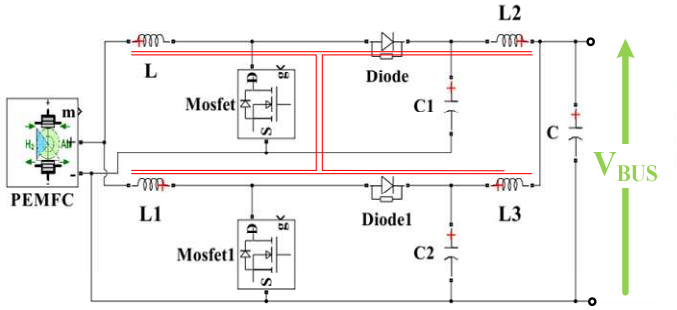

(b) IICIB by [46]

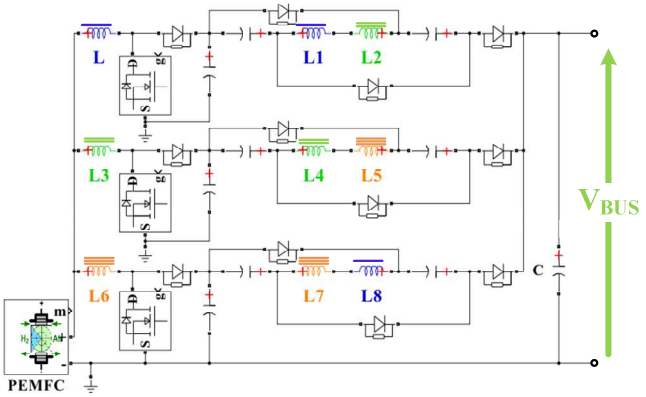

(c) 3-phase coupled IBC with voltage multiplier circuit by [52]

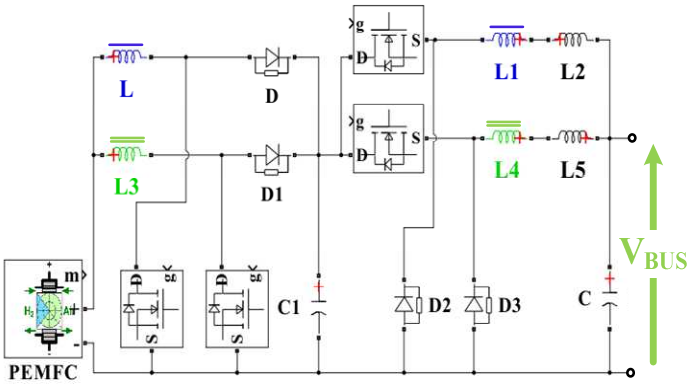

(d) 2-phase IB-BC by [51]

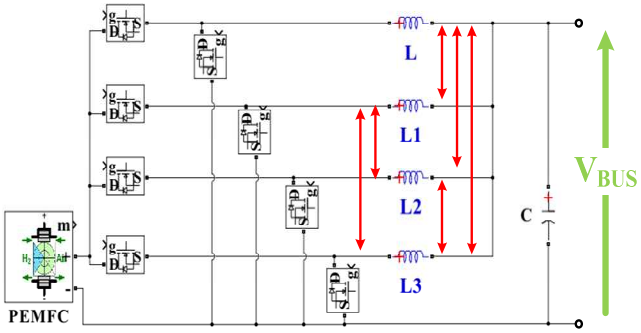

(e) 4-phase BIB/BC by [56]

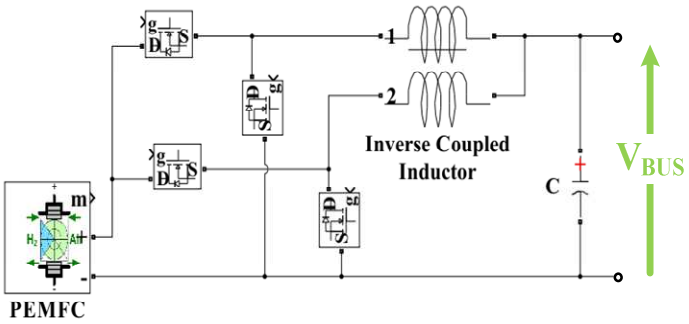

(f) 2-phase BIB/BC by [55]

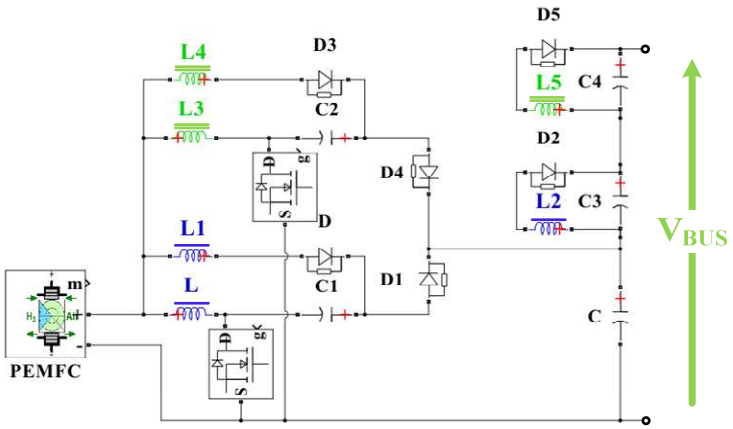

(g) Interleaved forward-flyback by [54]

Fig. 5.Schematics of non-isolated DC/DC converters for FCEVs application based on the coupled inductors

3.4. Power converters based on auxiliary voltage-boost circuit

In purpose of increasing the voltage gain ratio of conventional non-isolated converters, different kinds of auxiliary circuits are widely applied to this type of topologies. Table. IV presents the comparisons of non-isolated DC/DC converters integrated with the auxiliary voltage-boost structure; the topologies are presented in Fig. 6 respectively.

Table. IV. Comparisons of non-isolated DC/DC converters with auxiliary voltage-boost structure

Ref.	Voltage gain	Power level	Vin	Vout	Efficiency	Quantity of components	Special characteristic
[57]	2/(1-D)	1.6kW	50~120V	400V	~96.6%	7	Input-parallel Output-series boost converter.
[59]	$1/[(1-D_1)*(1-D_2)]$	200W	40V	300V	~90%	6	New Cascade boost converter.
[66]	$[(1+D)/(1-D)]^2$	--	12V	100V	<90%	12	3-Z-Network based boost converter.
[62]	2/(1-D)	3kW	20~35V	250V	~94%	8	2-phase IBC combined with switched capacitor.
[63]	2/(1-D)	1.2kW	26~43V	200V	~95%	8	2-phase IBC combined with voltage doubler circuit.
[64]	2/(1-D)	1kW	24V	250V	--	9	2-phase IBC combined with voltage double circuit.
[60]	2/(1-D)	100W	24V	240V	~95.8%	8	High step-up converter.
[67]	2/(3-4*D)	1.2kW	60~150V	400V	~95.66%	10	Three level Q-Z source boost converter.

The Input-Parallel Output-Series structure is interesting to be considered by the conventional Boost converter according to the study of Wang et al. [57]. An interleaved structure based on two inductors is chosen on the input side of this structure to reduce input current ripple. In addition, the two capacitors at the output side are connected in series to obtain a high voltage gain. Cascade Boost converter is another solution to achieve a high voltage gain ratio when the galvanic isolation is not necessary [58]. Nejad et al. [59] proposed a new cascade Boost converter; it can not only retain the advantages of the conventional cascade Boost converter but also reduce the conduction losses of semiconductors. Al-Saffar et al. [60] proposed a new single-switch step-up DC/DC converter which was derived from the conventional Boost converter integrated with self-lift Sepic converter for providing high voltage gain without extreme switch duty cycle.

Voltage Doubler Circuit (VDC) is well known due to its simple structure and principle. The basic operation of VDC has been discussed in detail by [61]. As presented in [62] [63] [64], some studies have integrated VDC with interleaved DC/DC converters in order to increase the voltage gain ratio. Fuzato et al. [64] analyzed the effect of the parasitic resistances on the static voltage gain of the 2-phase IBC combined with VDC using the final value theorem. Cardenas et al. [62] proposed a 3-kW DC-DC-AC power electronic interface for PEMFC application. A relatively high voltage gain (higher than 10 times) without transformer has been achieved. Wu et al. [63] proposed a power electronic interface based on a DC/DC converter and a DC/AC inverter which focused on grid-connected fuel cell generation system. In this study, the DC bus voltage has been set to 200V while the maximum input voltage was only 40V.

To realize a high voltage gain in DC/DC converters, Z-Source Impedance (ZSI) networks are also applied to boost the voltage due to the possibility of working in the shoot-through mode [65]. Zhang et al. [66] proposed a 3-Z-Network Boost converter that only utilized a single power switch; therefore easy to be controlled. The voltage gain could be higher than 9 times. Whereas, the maximum efficiency of the proposed converter was below 88% due to the high reverse recovery losses which are introduced by the high quantity of Si schottky

diodes. A Boost Three Level DC/DC Synchronous Rectification Q-Z source converter (BTL-SRqZ) has been proposed by Zhang et al. [67]. The advantages such as lower voltage stress for the power semiconductors, the common ground between the input and output sides, as well as the wide range of voltage-gain with modest duty cycles [0.5, 0.75] for the power switches have been achieved. In order to compare the voltage gains of each topology more clearly, the voltage gain ratios are calculated as the function of duty cycles as presented in Fig. 7.

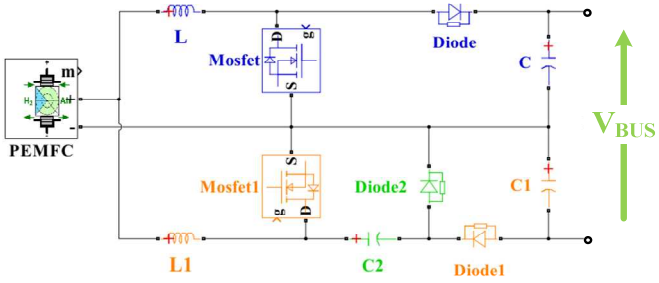

(a) Input-Parallel Output-Series DC/DC Boost converter by [57]

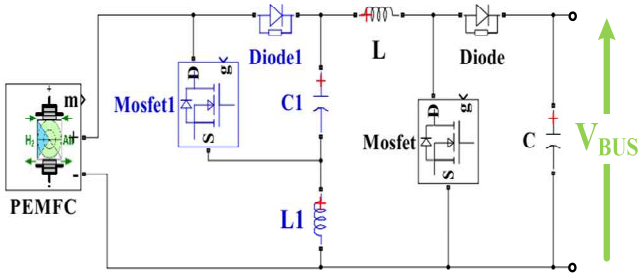

(b) Novel Cascade Boost converter by [59]

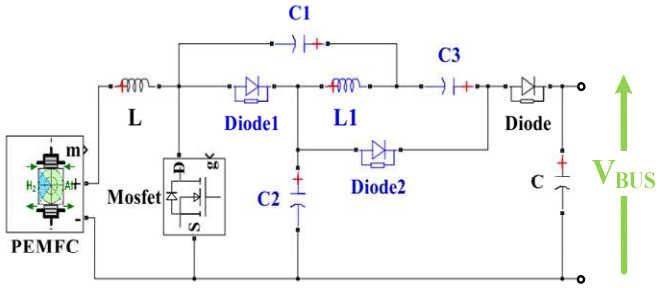

(c) Single-switch high step-up converter by [60]

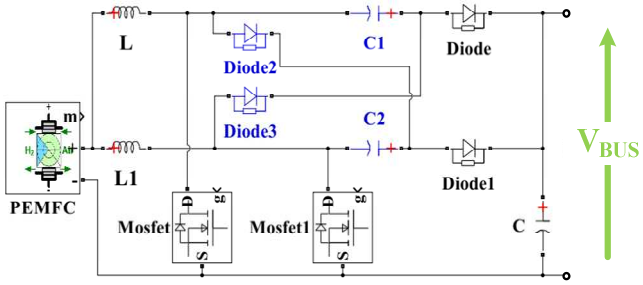

(d) IBC combined VDC by [62] [63] [64]

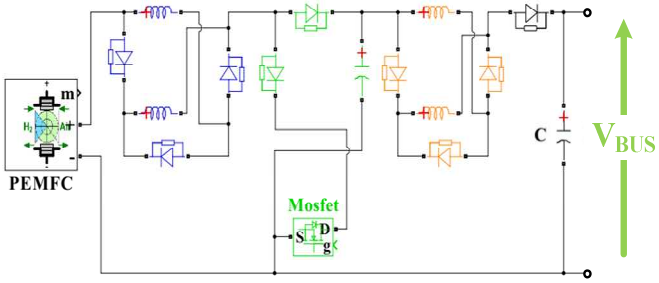

(e) 3-Z Network based Boost converter by [66]

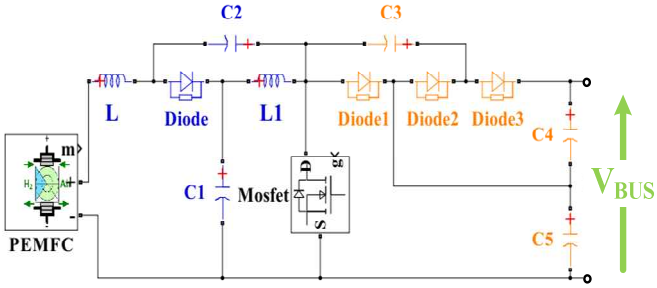

(f) Three level quasi-Z source based Boost converter by [67]

Fig. 6.Schematics of non-isolated DC/DC converters for FCEVs application integrated with the auxiliary voltage-boost circuit

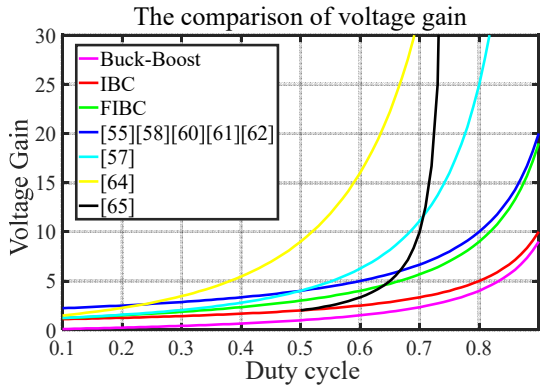

Fig. 7. The comparison of voltage gain ratio of the power converters combined with auxiliary voltage-boost circuit in an ideal case (without taking into account the internal resistance of inductors)

3.5. Summary

Generally, for the fuel cell electric vehicle applications, the input current ripple is closely related to the lifespan of a fuel cell stack. DC/DC converters based on interleaved structure (IBC, FIBC, etc.) can reduce the current ripple of the power source. Benefiting from

these specific topologies, the lifespan of fuel cell stack can be extended while the reliability can be increased [4][68]. Furthermore, the electric stresses of each component can be reduced. The new hybrid system of Toyota Mirai has currently a 4-phase interleaved boost converter between the fuel cell system and the motor drive system to step up the voltage from the fuel cell stack [13]. Benefiting from the developed converter, the voltage of the motor has been increased, the number of fuel cell single cells has been reduced, and the size and weight of the system have also been reduced. Therefore, the non-isolated DC/DC Boost converter based on interleaved structure is well-suited for FCEVs application.

Due to the limited inner space of a vehicle, a compact and light power conversion system is much more attractive. Generally speaking, the magnetic components (transformer and inductor) influence the total volume and weight significantly. High power application requires big transformers; however, the geometric sizing, the wound coil size and the difficulty of manufacturing will increase. Planar transformer technique is an attractive method to achieve a compact structure. Nevertheless, their prices are often very high, not really competitive for automotive applications. Towards non-isolated converters, to satisfy the requirement of low current ripple, big inductors are required. Interleaving structure is meaningful to reduce the current flowing through each inductor, thus the current ripple of inductor can be decreased. Another attractive approach is the coupled structure. A coupled inductor is a filter inductor having multiple windings and benefiting from this technique, the geometric sizing can be reduced and can induce the miniaturization of the heat dissipation system.

High switching frequency is also an effective method to reduce the magnetic component's volume. However, when the conventional Si semiconductor operates with high switching frequency (>20kHz), high switching loss and high reverse recovery losses will be separately introduced by MOSFET and diode. IGBT is possible for high current operating conditions, but to respect its inherent characteristics, the high switching frequency is not acceptable in many actual applications. SiC semiconductors have been developed rapidly in the last decade and already achieved commercialization. Low weight, small package, and interesting thermal performances made them attractive for FCEVs application. SiC MOSFET, which obtains high blocking voltage with low on-resistance and high speed switching with low capacitances, makes it possible to achieve higher system efficiency, reduce cooling requirements and increased power density. SiC schottky diode, which features high repetitive peak reverse voltage, zero reverse recovery current and high-frequency operation ability, makes it available to achieve high efficiency, zero switching losses and reduction of heat sink requirements. In general, the selection of SiC semiconductors can not only lead to a compact system but also increase system efficiency.

In consideration of the fuel cell characteristic (low-voltage high-current power source), a power converter which owns a high voltage gain ratio is more attractive. The isolated DC/DC boost converter can reach high voltage gains as discussed previously. However, compactness could be reduced. The conventional boost converter owns a medium voltage gain ratio. Different auxiliary circuits can be selected to increase the voltage gain significantly. Whereas a big quantity of additional components makes the system complicated, meanwhile the reliability of the system will be decreased by active components.

Efficiency is also an important factor to evaluate the performance of a power converter. Generally, power losses are mainly introduced by semiconductors and magnetic components. As analyzed previously, SiC-based semiconductor is an attractive approach to decrease power losses. GaN is another promising solution to improve the performances of semiconductors. Lower conduction resistance and higher switching frequency can be achieved by GaN semiconductor compared with the one based on SiC. However, the limitation of GaN semiconductor is that its blocking voltage is relatively low (<1000V) while higher cost is supported. Thus, currently, SiC semiconductor presents more advantages. On another side, core losses and copper losses are the dominating factors which decrease the efficiency of the magnetic component. Core loss is closely related to the core volume, the core material, and the geometric construction. High frequency is in favor of decreasing the core volume; hence, core loss can be reduced. Litz wire is suitable for high-frequency applications. Skin effect, which is an electromagnetic inherent characteristic, can be avoided by this special technique and thereby the copper losses can be reduced.

IV. On-line EIS detection based on DC/DC converter connected to the fuel cell stack

Load cycling is the main characteristic that affects PEMFC lifespan in FCEVs applications [69]. During the load changing process, the current density of fuel cell stack changes frequently. As a complex electrochemical power device [18], relative humidity, temperature, gas flow rate, partial pressure, and other factors can influence the fuel cell system performance significantly, and various faults possibly occur to PEMFC during the operating period. Short-circuit, which leads to the membrane and catalyst layer degradation, occurs in the microsecond or millisecond time range and is irreversible on-site [70]. Fuel starvation occurs in the millisecond or second time range, and will lead to the catalytic layer degradation [71]. Flooding and drying, which occur most commonly during operations, can lead to the performance reduction of the fuel cell system. Flooding can increase the fuel cell system degradation as a result of starvation and material

alteration [72]; drying can result in pinhole degradation of the polymer membrane [73]. Both flooding and drying are entirely reversible by timely treatments. CO poisoning also leads to fuel cell system performance losses, and the reversibility closely relates to the exposure time, temperature and in-channel gas composition [74]. Fig. 8 presents a schematization of the most frequent faults in a PEMFC based on different response times. Therefore, fault diagnostic methods are important to be developed in order to expand fuel cell lifespan. Different fault diagnostic methods for the fuel cell system are discussed in the subsections, and available studies of the on-line EIS detection are reviewed. A design guideline of the on-line EIS detection integrated with the fuel cell connected DC/DC converter is proposed.

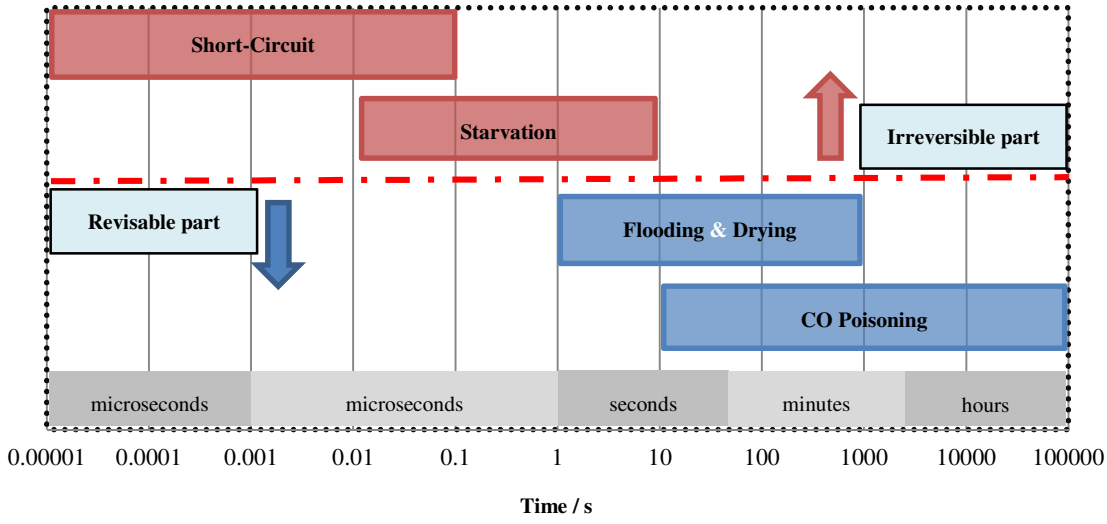

Fig. 8. Illustration of the most common faults of a PEMFC based on response times

4.1. Fault diagnostic methods of the fuel cell system

In recent years, diverse techniques and methods have been developed for PEMFC's diagnosis. These diagnostic approaches are generally classified into two types: model-based ones [75] and non-model based ones [76].

The model-based diagnosis is based on the development of a model which is capable of reflecting the status of the monitored system. Regarding the model-based approach, the fault diagnosis is commonly accomplished by residual evaluation where a residual inference is used for possible fault occurrence detection [77]. Hence, such a method is also referred to as the residual-based diagnosis. The physical multidimensional models are presented as a series of algebraic and/or differential equations. A high computational effort is required to obtain the solution, which means a near impossibility for real-time or on-line application [78]. The “black-box” model, which is directly derived from experiments, requests low computational efforts and is attractive for non-linear monitoring applications. However, this kind of model is strongly depending on available experiments which can reduce its genericity [79]. Therefore, the combination of these two model-based methods can simplify the characterization of a system, replace some complex mathematical equations, and reduce the requirement of computational effort [80].

Compared with model-based approaches, non-model based methods could be divided into knowledge-based and signal-based. The objective of this kind of methods is to detect, isolate, and classify different types of faults based on signal processing or heuristic knowledge or a combination of both. Artificial Intelligence (AI) methods have attracted a lot of attention in the field of diagnosis because they are effective in the identification of fault patterns without system structure knowledge. Neural network (NN), Fuzzy logic (FL), and Neural-fuzzy method are mostly used in this field. NN achieves the ability to handle noisy data [81] while FL is possible to handle the uncertainty in the system [82]. A neural-fuzzy method combines the advantages of NN and FL, and better generalization capability is obtained compared with NN [83]. Statistical methods such as Principle Component Analysis (PCA), Fisher Discriminant Analysis (FDA), Bayesian network (BN) and others are the most frequently used variable dimension-reduction methods to extract the most discriminating features from a huge amount of data [84]. Signal processing methods are effective to analyze oscillations of the detected signals. Fast Fourier Transform (FFT) and Wavelet Transform (WT) are commonly used and they can provide a view of signals in the frequency domain [85]. However, the main drawback of model-based methods is the requirement of huge amounts of data sets that originally acquired on a system in day-to-day use or on a dedicated laboratory test bench. Moreover, these data sets must be acquired under both normal and targeted fault conditions [3].

Towards FCEVs applications, the requirement of the fuel cell diagnostic method can be summarized as high accuracy, high robustness,

quick response, high sensitivity, and good versatility. At the same time, the diagnostic method is also requested to have the possibility of on-line or onboard application, and with minimum dependence of sensor or other additional equipment.

4.2. The applications of EIS

Electrochemical impedance spectroscopy (EIS) is established as a powerful characterization tool to detect different failure mechanisms occurring in the fuel cell system. Impedance spectra can help to characterize a cell in a much more efficient mode than just analyzing the polarization curve [86]. Many works highlight the use of the EIS technique for the fuel cell parameter identification, which is a kind of model-based diagnosis method and is effective for both fault detection and isolation [87]. EIS technique is also treated as an efficient means for non-model based diagnosis method because it helps a lot for pre-processing the original data sets and for decreasing the misclassification rate [88]. Some typical applications of the EIS technique as a fault diagnostic approach for the fuel cells are presented in Table. V.

Table. V. Applications of EIS technique as a fault diagnostic method for the fuel cells

Ref.	Description of the method	Fault types	EIS achievement	On/off-line
[89]	Use EIS estimate the high-frequency impedance data and the parameters characterizing the cathode reaction of H_2/air fed PEMFC.	No information.	Labview program based.	Off-line & In-lib
[90]	Use EIS technique as the diagnostic approach to two PEMFC failures associated with low-frequency current ripple.	Cathode flooding; Membrane drying.	EIS spectrometer (Zahner, IM6ex). Range from 2kHz to 0.03Hz.	Off-line & In-lib
[91]	Use EIS study impacts of operating conditions on the effects of chloride contamination on PEMFC.	Increase charge transfer resistance and mass transfer resistance.	EIS spectrometer (Teledyne test station). Range from 3kHz to 0.1Hz.	Off-line & In-lib
[92]	Use EIS study DMFC's electrochemical process and degradation reasons.	Ru's dispersing; MEA's swelling; Cathode's water flooding.	VMP2 electrochemical workstation (Bio-logic).	Off-line & In-lib
[93]	Combine EIS and SANS techniques to study water management of PEMFC in operando at sub-zero temperatures.	Member dehydration.	Bio-Logic VSP impedance meter.	Off-line & In-lib
[94]	Use EIS reveal the degradation phenomena caused by cell polarity reversal due to fuel starvation of PEMFC.	Fuel starvation.	Frequency response analyzer from Solartron Model 1250.	Off-line & In-lib
[95]	Use spatial EIS and current distribution model study the effect of low concentration CO poisoning of Pt anode in PEMFC.	Anode CO poisoning.	Hawaii Natural Energy Institute's (HNEI) segmented cell system.	Off-line & In-lib
[96]	Use EIS study the influence of CO and methanol vapor contamination of the anode gas in a HT-PEMFC.	Anode poisoning (CO and methanol vapor).	Gamry Reference 3000 instrument.	Off-line & In-lib
[97]	Use EIS assess the effect of different MEA conditionings for PEMFC performance.	In fact, different operating conditions of PEMFC have been studied in this paper. But they can't be called as faults.	Fuel cell test station: Scribner, 850e	Off-line & In-lib
[98]	Use EIS analyze geometrical features of PEMFC based on computational fluid dynamics.	No information.	Electronic load CHROMA 63600. Range from 20kHz to 0.05Hz.	Off-line & In-lib

Mainka et al. [89] made a discussion on the estimation of impedance parameters of H_2/air fed PEMFC. The parameters characterizing charge separation and transport process at the cathode can thus be estimated with the high-frequency impedance data, independently of the oxygen transport model. Consequently, even in the absence of fully validated oxygen transport impedance, EIS can be used as an alternative method for the estimation of the parameters characterizing the cathode reaction. Kim et al. [90] dealt with a diagnosis of cathode flooding and membrane drying associated with a low-frequency ripple current of a PEMFC based on EIS analysis. Specifically, it has been shown that a low-frequency ripple current more accelerates the PEMFC degradation with these two PEMFC failures. Li et al. [91] used EIS as a diagnostic tool in purpose of exploring changes in cell component resistances during the contamination tests because the chloride contaminated fuel and/or air streams in an operating PEMFC can cause significant adverse effects on fuel cell performance and durability. Wang et al. [92] have successfully investigated direct methanol fuel cell's (DMFC's) electrochemical process in situ using the EIS method. The results showed that Ru's dispersing, membrane's swelling and water flooding were the main reasons resulting in performance decline. Morin et al. [93] combined Small-Angle Neutron Scattering (SANS) and EIS techniques to study the water management in an operating PEMFC at sub-zero temperatures. It was shown that the fuel cell operation at sub-zero temperature can be

conducted in operando by SANS meanwhile the variation of membrane water content can be confirmed by EIS technique with different current density. Travassos et al. [94] used the EIS technique to report the degradation phenomena caused by cell polarity reversal due to the fuel starvation of an open cathode membrane electrode assembly. Reshetenko et al. [95] studied the effects of CO on PEMFC performance with a segmented cell by the spatial EIS technique. The spatial EIS data were analyzed using the equivalent electric circuits approach. A current distribution model and the EIS interpolation method were applied for detailed analysis. Jeppesen et al. [96] have presented a comprehensive mapping of electrochemical impedance measurements under the influence of CO and methanol vapor contamination of the anode gas in a high-temperature PEMFC (HT-PEMFC), at varying load current. Zhiani et al. [97] have studied the effects of three different commonly used on-line membrane-electrode assembly (MEA) conditioning procedures on the final MEA performance, and the performance of activated PEMFCs was investigated under different operation conditions (low and high relative humidity, low and high cell pressure and low and high oxidant concentration) by EIS technique. Baricci et al. [98] have made use of EIS for the design of PEMFC's flow field geometry because EIS allows separating the effect of electric resistance due to contact between GDL and bipolar plates, electrode kinetics oxygen transport under the rib. Advanced understanding of EIS features that has been detailed in this work could be also beneficial for the implementation of EIS as a diagnostic measurement on-board to manage the operating conditions and detect faults.

Although EIS has already been widely applied for the fuel cell in-lab/off-line applications, the acquisition of data-sets is mainly based on impedance meter equipment and fuel cell test station which are impossible for onboard/on-line applications. Thus, the realization of on-line EIS detection is quite important and urgent nowadays for FCEVs application.

4.3. On-line EIS realization based on the power converter

Classically, a DC/DC converter is considered for the connection between the fuel cell stack and the DC bus, in order to realize the power conversion. The ripple frequency of a DC/DC converter is just the same as the switching frequency of the power switching semiconductors such as power MOSFET. This provides a favorable crucible for the fuel cell system diagnosis without any other additional equipment to respect the limited space in a FCEV [99]. Table. VI. presents a review of the realizations of EIS detection based on actual power converters. As common electrochemical and electrostatic energy storage devices, battery and super-capacitor are also be analyzed with this approach.

Table. VI. Comparisons of EIS detection based on the practical converter connected to the power source

Application field	Converter type	Ref.	Control strategy & Controlled object	Control during detection	Input current ripple	Perturbation injection method
PEMFC	Boost	[100]	PID controller.	--	High	--
		[103]	Dual-loop PI controller. DC bus voltage and input current.	Close loop		Injected current or voltage perturbation.
		[104]	Dual-loop PI controller.	--		--
	IBC	[26]	Sliding-Mode controller. DC bus voltage and inductor current.	Close loop	Low	Injected current perturbation.
	Full bridge	[101]	PI controller. DC bus voltage.	Open loop	High	Injected current perturbation.
		[7]	PI controller. DC bus voltage.	Open loop		Injected current perturbation.
Battery	Boost	[105]	--	Open loop	High	Injected duty cycle perturbation.
	Full bridge	[102]	Dual-loop PI controller. Output voltage and output current.	--		--
PEMFC & EDLC	Boost	[106]	Dual-loop PI controller. DC bus voltage and source voltage.	--		Injected voltage perturbation.
DC Capacitive Network	Buck-Boost	[107]	Dual-loop PI controller. DC bus voltage and battery current.	Open loop	--	Injected current perturbation.

Narjiss et al. [101] and Depernet et al. [7] consisted of on-line detection of fuel cell dysfunction thanks to the selected full bridge converter without additional hardware component. The switching frequency was relatively high (50kHz), but the semiconductors were

conventional Si material which increased switching losses at this operating condition. Doan et al. [102] have designed an intelligent charger which was a full bridge converter combined with a controlled rectifier, and the on-line battery diagnosis function has been realized. The relationship between the perturbation signal frequency and the control loop bandwidth was mentioned. The nonlinear least square fitting algorithm was utilized to estimate battery parameters.

Conventional Boost converter was selected by [100] [103] [105] and [104] to realize EIS detection of electrochemical sources. The method utilized by Hinaje et al. [100] relied on the estimation of the internal resistance calculated from the voltage and current ripples, thus, on-line humidification diagnosis of PEMFC was realized. However, the real and imaginary parts of the AC impedance cannot be analyzed separately. Bethoux et al. [103] have studied the stability of the control system during EIS detection. Relied on this study, injection of the perturbation signal into the fuel cell current reference or the DC bus voltage reference is depending on its frequency. Hong et al. [104] detected EIS of PEMFC based on two parallel Boost converters and a battery was connected to DC bus directly. To control the input current, a control scheme of two-degrees of freedom was put forward. In the outer control loop, a PI controller and a look-up table were used to set the reference value of the output current. The look-up table got the output power of the stack according to the reference output current. In the inner loop, the output current was controlled based on the state space model of the converter. To decrease the input current overshoot, the feedforward control was added to the duty cycle. The output voltage of this converter was determined by the battery. Varnosfaderani et al. [105] presented an on-line impedance estimation approach for the battery application. A small component representing a low-frequency component was directly imposed to the duty cycle when the system operated under steady state. The ripple and harmonics of battery voltage and current were separately analyzed.

Depending on the study of Katayama et al. [106], the diode of the conventional Boost converter was replaced by a MOSFET. The proposed circuit was based on two power sources: PEMFC and EDLC. Each power source was connected with its own Boost converter. The control strategy of EDLC converter is DC bus voltage control. The control strategy of PEMFC converter is dual loop voltage control: the outer loop is EDLC voltage control, and the inner loop is FC voltage control. During the diagnosis mode, a sinusoid signal with a certain frequency and amplitude is injected to the FC converter reference. However, the perturbation of the DC bus voltage has been introduced while the input current ripple was high. Depernet et al. [107] integrated the EIS detection functionality of lead-acid batteries with a Buck-Boost converter for storage management of standalone power plant.

As discussed previously, input current ripple influences fuel cell stack's lifespan a lot. However, among these references, conventional DC/DC (Boost, Buck-Boost) or DC/AC/DC (Full-Bridge) converters were mainly considered. Thus, the fuel cell current ripple was still kept at a high level. Furthermore, Si semiconductors were utilized which means poor performances under high switching condition, especially high switching losses of MOSFET and high reverse recovery losses of Schottky diode. In [101], [107], [105] and [7], open loop control were applied during EIS detection process. The stability of DC bus voltage cannot be ensured during this period.

Wang et al. [26] currently proposed on-line detection of impedance spectroscopy for PEMFC application based on connected electric power converter. The proposed converter based on high switching frequency, SiC semiconductors and inverse coupled inductors is an innovative solution to settle the problem of regulating PEMFC voltage to satisfy the voltage requirement of the fuel cell electric vehicle DC bus. Compared with the existing studies, the proposed strategy has been verified by FC stack Randles model in a wide range of frequencies (maximum 10kHz). Besides, the selected Sliding-Mode Control can well regulate the fuel cell current and DC bus voltage and realize close loop control either under nominal operating conditions or disturbed conditions.

In general, these following features are essential for a DC/DC converter, which is focused on FCEV application meanwhile integrated with EIS detection ability:

Table. VII. Requirements for a DC/DC converter focused on FCEV application combined with EIS on-line detection functionality

Required feature	Approaches
High reliability	● Use proper topology to reduce input current ripple in purpose of extending fuel cell stack's lifespan; ● Select proper semiconductor which achieves good thermal performance; ● Realize close loop control during EIS detection period to ensure the stability of DC bus voltage.
High power density	● Optimize magnetic component structure to minimize total volume and weight; ● Select high switching frequency to minimize magnetic component; ● Replace power IGBT module by advanced power MOSFET to reduce semiconductors' volumes, meanwhile compact heat sink can be utilized.
High energy efficiency	● Semiconductor based on SiC material is attractive to reduce power losses; ● Auxiliary soft-switching circuit can be selected to reduce switching losses; ● Magnetic component with compact structure is promising to decrease core losses.

V. Conclusion

In this paper, a review focusing on the integration of EIS detection functionality in DC/DC converter for FCEV applications is presented.

The non-isolated DC/DC converter and the isolated DC/AC/DC converter are commonly considered. The characteristics like high compactness, simple structure and low cost are achieved by the non-isolated topologies. However, the voltage gain ratio of this type of topology is relatively low. Although different auxiliary circuits can be selected to increase the voltage gain ratio, the complexity of the converter will be increased while the reliability will be decreased due to the application of additional components. High voltage gain ratio can be achieved easily by the isolated converters due to the magnetic transformer. The voltage gain ratio of this kind of topology is closely related to the turn ratio of transformer. But the compactness of the converter will be decreased. Another approach to achieve a high voltage gain ratio is replacing the conventional inductors by the ones based on a coupled structure. Meanwhile, the total volume of the magnetic component can be reduced. The current ripple of the fuel cell stack influences its lifespan a lot; therefore, the interleaved structure is attractive to reduce the input current ripple while the lifespan of the power source can be extended. Meanwhile, the redundancy of the converter can also be improved by this specific structure. To decrease the power losses introduced by the semiconductors, the ones manufactured by Wide Band-Gap (WBG) materials such as Silicon Carbide (SiC) and Gallium Nitride (GaN) are treated as a promising solution. Better thermal performance, lower switching losses and lower conduction losses can be achieved. The efficiency can be improved and the cooling system can be simplified.

As discussed in the previous section, fault diagnosis is essential for the fuel cell system both in the laboratory and in actual applications. Electrochemical Impedance Spectroscopy (EIS) is one of the most promising diagnostic approaches to handle this issue. Due to the limited inner space of a vehicle, on-line EIS detection functionality integrated with the DC/DC converter which is connected to the fuel cell stack is a promising approach. Benefiting from this method, no additional equipment is required. Some efforts have been done by others to realize this diagnostic method as demonstrated in this paper. Nevertheless, the topologies utilized in these researches were the conventional ones which didn't achieve the ability to reduce the input current ripple. Meanwhile, in some studies, the converters were in open-loop control mode during on-line EIS detection processes. The stability of DC bus voltage can't therefore be ensured.

Therefore, concerning the fuel cell electric vehicle applications, a DC/DC boost converter which achieves low input current ripple, compact structure, high voltage gain ratio, high efficiency and high redundancy is attractive for the practical application. After the power conversion has been realized, the integration of the EIS detection process with the proposed power conditioning unit is a promising approach to realize on-line water management of the fuel cell stack without any additional equipment.

References

[1] Daud, W. R. W., Rosli, R. E., Majlan, E. H., Hamid, S. A. A., Mohamed, R., & Husaini, T. (2017). PEM fuel cell system control: A review. Renewable Energy, 113, 620-638.

[2] Department of Energy US. Fuel Economy; 2017.

[3] Hissel, D., & Péra, M. C. (2016). Diagnostic & health management of fuel cell systems: Issues and solutions. Annual Reviews in Control, 42, 201-211.

[4] Wahdame, B., Girardot, L., Hissel, D., Harel, F., François, X., Candusso, D., ... & Dumercy, L. (2008, June). Impact of power converter current ripple on the durability of a fuel cell stack. In Industrial Electronics, 2008. ISIE 2008. IEEE International Symposium on (pp. 1495-1500). IEEE.

[5] https://global.honda/innovation/FuelCell/Clarity-Fuel-Cell-engineer-talk.html; 2019.

[6] Niya, S. M. R., & Hoorfar, M. (2013). Study of proton exchange membrane fuel cells using electrochemical impedance spectroscopy technique–A review. Journal of Power Sources, 240, 281-293.

[7] Depernet, D., Narjiss, A., Gustin, F., Hissel, D., & Péra, M. C. (2016). Integration of electrochemical impedance spectroscopy functionality in proton exchange membrane fuel cell power converter. International Journal of Hydrogen Energy, 41(11), 5378-5388.

[8] https://www.fueleconomy.gov/feg/pdfs/guides/FEG2019.pdf; 2019.

[9] Wand, G. (2006). Fuel cell history, Part 2. Fuel Cell Today, Archive Article, 2006-06.

[10] https://www.fueleconomy.gov; 2019.

[11] https://blog.toyota.co.uk/toyota-mirai-technical-specifications-vs-fchv-adv; 2019.

[12] https://www.toyota-global.com/innovation/environmental_technology/technology_file/fuel_cell_hybrid/fcstack.html; 2019.

[13] Hasuka, Y., Sekine, H., Katano, K., & Nonobe, Y. (2015). Development of boost converter for MIRAI(No. 2015-01-1170). SAE Technical Paper.

[14] https://www.hs-karlsruhe.de/fileadmin/hska/EIT/Aktuelles/seminar_erneurbare_energien/Sommer_2017/Folien/140617Honda.pdf; 2019.
[15] https://www.wolfspeed.com/power/products/sic-power-modules;2019
[16] https://h2tools.org/sites/default/files/ix35%20FCEV%20ERG_Eng.pdf; 2019.
[17] http://www.ehec.info/images/EHEC2018/Plenaries/EHEC2018_Hyundai_Arboleda.pdf; 2019
[18] Barbir, F. (2006). PEM fuel cells. In Fuel Cell Technology (pp. 27-51). Springer, London.
[19] Péra, M. C., Hissel, D., Gualous, H., & Turpin, C. (2013). Basic Concepts of Electrochemistry used in Electrical Engineering. Electrochemical Components, 1-40.
[20] http://www.hydrogenandfuelcells.energy.gov.;2019
[21] Das, H. S., Tan, C. W., & Yatim, A. H. M. (2017). Fuel cell hybrid electric vehicles: A review on power conditioning units and topologies. Renewable and Sustainable Energy Reviews, 76, 268-291.
[22] Kirubakaran, A., Jain, S., & Nema, R. K. (2009). A review on fuel cell technologies and power electronic interface. Renewable and Sustainable Energy Reviews, 13(9), 2430-2440.
[23] Das, V., Padmanaban, S., Venkitusamy, K., Selvamuthukumaran, R., Blaabjerg, F., & Siano, P. (2017). Recent advances and challenges of fuel cell based power system architectures and control–A review. Renewable and Sustainable Energy Reviews, 73, 10-18.
[24] Tani, A., Camara, M. B., & Dakyo, B. (2012). Energy management based on frequency approach for hybrid electric vehicle applications: Fuel-cell/lithium-battery and ultracapacitors. IEEE Transactions on Vehicular Technology, 61(8), 3375-3386.
[25] Wang, Y. X., Yu, D. H., & Kim, Y. B. (2014). Robust time-delay control for the DC–DC boost converter. IEEE Transactions on Industrial Electronics, 61(9), 4829-4837.
[26] Wang, H., Gaillard, A., & Hissel, D. (2019). Online electrochemical impedance spectroscopy detection integrated with step-up converter for fuel cell electric vehicle. International Journal of Hydrogen Energy, 44(2), 1110-1121.
[27] Zhang, L., Xu, D., Shen, G., Chen, M., Ioinovici, A., & Wu, X. (2015). A high step-up DC to DC converter under alternating phase shift control for fuel cell power system. IEEE Transactions on Power Electronics, 30(3), 1694-1703.
[28] Thounthong, P., & Davat, B. (2010). Study of a multiphase interleaved step-up converter for fuel cell high power applications. Energy Conversion and Management, 51(4), 826-832.
[29] Wen, H., & Su, B. (2016). Hybrid-mode interleaved boost converter design for fuel cell electric vehicles. Energy Conversion and Management, 122, 477-487.
[30] Benyahia, N., Denoun, H., Badji, A., Zaouia, M., Rekioua, T., Benamrouche, N., & Rekioua, D. (2014). MPPT controller for an interleaved boost dc–dc converter used in fuel cell electric vehicles. International journal of hydrogen energy, 39(27), 15196-15205.
[31] Huangfu, Y., Zhuo, S., Chen, F., Pang, S., Zhao, D., & Gao, F. (2017). Robust Voltage Control of Floating Interleaved Boost Converter for Fuel Cell Systems. IEEE Transactions on Industry Applications.
[32] Kabalo, M., Paire, D., Blunier, B., Bouquain, D., Simões, M. G., & Miraoui, A. (2012). Experimental validation of high-voltage-ratio low-input-current-ripple converters for hybrid fuel cell supercapacitor systems. IEEE Transactions on Vehicular Technology, 61(8), 3430-3440.
[33] Gao, D., Jin, Z., Liu, J., & Ouyang, M. (2016). An interleaved step-up/step-down converter for fuel cell vehicle applications. International Journal of Hydrogen Energy, 41(47), 22422-22432.
[34] Han, D., & Sarlioglu, B. (2016). Deadtime effect on GaN-based synchronous boost converter and analytical model for optimal deadtime selection. IEEE Transactions on Power Electronics, 31(1), 601-612.
[35] Roccaforte, F., Fiorenza, P., Greco, G., Vivona, M., Nigro, R. L., Giannazzo, F., ... & Saggio, M. (2014). Recent advances on dielectrics technology for SiC and GaN power devices. Applied Surface Science, 301, 9-18.
[36] Schrock, J. A., Pushpakaran, B. N., Bilbao, A. V., Ray, W. B., Hirsch, E. A., Kelley, M. D., ... & Bayne, S. B. (2016). Failure analysis of 1200-V/150-A SiC MOSFET under repetitive pulsed overcurrent conditions. IEEE Trans. Power Electron., 31(3), 1816-1821.
[37] Kreutzer, O., Billmann, M., Maerz, M., & Lange, A. (2016, November). Non-isolating DC/DC converter for a fuel cell powered aircraft. In Electrical Systems for Aircraft, Railway, Ship Propulsion and Road Vehicles & International Transportation Electrification Conference (ESARS-ITEC), International Conference on (pp. 1-6). IEEE.
[38] Kreutzer, O., Gerner, M., Billmann, M., & Maerz, M. (2018, June). A 3.6 kV full SiC fuel cell boost converter for high power electric aircraft. In 2018 IEEE Transportation Electrification Conference and Expo (ITEC) (pp. 220-225). IEEE.
[39] Masrur, M. A. (2016). Toward ground vehicle electrification in the US Army: an overview of recent activities. IEEE Electrification Magazine, 4(1), 33-45.

[40] Elsayad, N., Moradisizkoohi, H., & Mohammed, O. A. (2018, October). A Three-Level Boost Converter with an Extended Gain and Reduced Voltage Stress using WBG Devices. In 2018 IEEE 6th Workshop on Wide Bandgap Power Devices and Applications (WiPDA) (pp. 45-50). IEEE.

[41] Han, D., Noppakunkajorn, J., & Sarlioglu, B. (2014). Comprehensive efficiency, weight, and volume comparison of SiC-and Si-based bidirectional DC–DC converters for hybrid electric vehicles. IEEE Transactions on vehicular technology, 63(7), 3001-3010.

[42] Ding, X., Du, M., Zhou, T., Guo, H., & Zhang, C. (2017). Comprehensive comparison between silicon carbide MOSFETs and silicon IGBTs based traction systems for electric vehicles. Applied energy, 194, 626-634.

[43] Olejniczak, K., Flint, T., Simco, D., Storkov, S., McGee, B., Shaw, R., ... & McNutt, T. (2017, March). A compact 110 kVA, 140 C ambient, 105 C liquid cooled, all-SiC inverter for electric vehicle traction drives. In Applied Power Electronics Conference and Exposition (APEC), 2017 IEEE (pp. 735-742). IEEE.

[44] Dang, Z., & Qahouq, J. A. A. (2017). Permanent-Magnet Coupled Power Inductor for Multiphase DC–DC Power Converters. IEEE Transactions on Industrial Electronics, 64(3), 1971-1981.

[45] Barry, B. C., Hayes, J. G., & Ryłko, M. S. (2015). CCM and DCM operation of the interleaved two-phase boost converter with discrete and coupled inductors. IEEE Transactions on Power Electronics, 30(12), 6551-6567.

[46] Liu, H., & Zhang, D. (2017). Two-phase interleaved inverse-coupled inductor boost without right half-plane zeros. IEEE Transactions on Power Electronics, 32(3), 1844-1859.

[47] Martinez, W., Cortes, C., Yamamoto, M., Imaoka, J., & Umetani, K. (2017). Total volume evaluation of high-power density non-isolated DC–DC converters with integrated magnetics for electric vehicles. IET Power Electronics, 10(14), 2010-2020.

[48] Barry, B. C., Hayes, J. G., Rylko, M. S., Stala, R., Penczek, A., Mondzik, A., & Ryan, R. T. (2018). Small-Signal Model of the Two-Phase Interleaved Coupled-Inductor Boost Converter. IEEE Transactions on Power Electronics, 33(9), 8052-8064.

[49] Imaoka, J., Okamoto, K., Kimura, S., Noah, M., Martinez, W., Yamamoto, M., & Shoyama, M. (2018). A Magnetic Design Method Considering DC-Biased Magnetization for Integrated Magnetic Components Used in Multiphase Boost Converters. IEEE Transactions on Power Electronics, 33(4), 3346-3362.

[50] Chen, Y. T., Li, Z. M., & Liang, R. H. (2018). A novel soft-switching interleaved coupled-inductor boost converter with only single auxiliary circuit. IEEE Transactions on Power Electronics, 33(3), 2267-2281.

[51] Samavatian, V., & Radan, A. (2015). A high efficiency input/output magnetically coupled interleaved buck–boost converter with low internal oscillation for fuel-cell applications: Small signal modeling and dynamic analysis. International Journal of Electrical Power & Energy Systems, 67, 261-271.

[52] Nouri, T., Hosseini, S. H., Babaei, E., & Ebrahimi, J. (2016). A non-isolated three-phase high step-up DC–DC converter suitable for renewable energy systems. Electric Power Systems Research, 140, 209-224.

[53] Zhang, Z. (1987). Coupled-inductor magnetics in power electronics (Doctoral dissertation, California Institute of Technology).

[54] Tseng, K. C., Chen, J. Z., Lin, J. T., Huang, C. C., & Yen, T. H. (2015). High step-up interleaved forward-flyback boost converter with three-winding coupled inductors. IEEE Transactions on Power Electronics, 30(9), 4696-4703.

[55] Huang, X., Lee, F. C., Li, Q., & Du, W. (2016). High-frequency high-efficiency GaN-based interleaved CRM bidirectional buck/boost converter with inverse coupled inductor. IEEE Transactions on Power Electronics, 31(6), 4343-4352.

[56] Yang, Y., Guan, T., Zhang, S., Jiang, W., & Huang, W. (2018). More Symmetric Four-Phase Inverse Coupled Inductor for Low Current Ripples & High-Efficiency Interleaved Bidirectional Buck/Boost Converter. IEEE Transactions on Power Electronics, 33(3), 1952-1966.

[57] Wang, P., Zhou, L., Zhang, Y., Li, J., & Sumner, M. (2017). Input-parallel Output-series DC-DC Boost Converter with a Wide Input Voltage Range, for Fuel Cell Vehicles. IEEE Transactions on Vehicular Technology.

[58] García, O., Cobos, J. A., Prieto, R., Alou, P., & Uceda, J. (2003). Single phase power factor correction: A survey. IEEE Transactions on Power Electronics, 18(3), 749-755.

[59] Nejad, M. L., Poorali, B., Adib, E., & Birjandi, A. A. M. (2016). New cascade boost converter with reduced losses. IET Power Electronics, 9(6), 1213-1219.

[60] Al-Saffar, M. A., & Ismail, E. H. (2015). A high voltage ratio and low stress DC–DC converter with reduced input current ripple for fuel cell source. Renewable Energy, 82, 35-43.

[61] Gules, R., Pfitscher, L. L., & Franco, L. C. (2003, June). An interleaved boost DC-DC converter with large conversion ratio. In Industrial Electronics, 2003. ISIE'03. 2003 IEEE International Symposium on (Vol. 1, pp. 411-416). IEEE.

[62] Cardenas, A., Agbossou, K., & Henao, N. (2015). Development of power interface with FPGA-based adaptive control for PEM-FC system. IEEE Transactions on Energy Conversion, 30(1), 296-306.

[63] Wu, J. C., Wu, K. D., Jou, H. L., Wu, Z. H., & Chang, S. K. (2013). Novel power electronic interface for grid-connected fuel cell power generation system. Energy conversion and management, 71, 227-234.

[64] Fuzato, G. H., Aguiar, C. R., Ottoboni, K. D. A., Bastos, R. F., & Machado, R. Q. (2016). Voltage gain analysis of the interleaved boost with voltage multiplier converter used as electronic interface for fuel cells systems. IET Power Electronics, 9(9), 1842-1851

[65] Ge, B., Lei, Q., Qian, W., & Peng, F. Z. (2012). A family of Z-source matrix converters. IEEE Transactions on Industrial Electronics, 59(1), 35-46.

[66] Zhang, G., Zhang, B., Li, Z., Qiu, D., Yang, L., & Halang, W. A. (2015). A 3-Z-Network Boost Converter. IEEE Transactions on Industrial Electronics, 1(62), 278-288.

[67] Zhang, Y., Shi, J., Zhou, L., Li, J., Sumner, M., Wang, P., & Xia, C. (2017). Wide Input-Voltage Range Boost Three-Level DC–DC Converter With Quasi-Z Source for Fuel Cell Vehicles. IEEE Transactions on Power Electronics, 32(9), 6728-6738.

[68] Kolli, A., Gaillard, A., De Bernardinis, A., Bethoux, O., Hissel, D., & Khatir, Z. (2015). A review on DC/DC converter architectures for power fuel cell applications. Energy Conversion and Management, 105, 716-730.

[69] Pei, P., & Chen, H. (2014). Main factors affecting the lifetime of Proton Exchange Membrane fuel cells in vehicle applications: A review. Applied Energy, 125, 60-75.

[70] Silva, R. E., Harel, F., Jemei, S., Gouriveau, R., Hissel, D., Boulon, L., & Agbossou, K. (2014). Proton Exchange Membrane Fuel Cell Operation and Degradation in Short-Circuit. Fuel Cells, 14(6), 894-905.

[71] Yousfi-Steiner, N., Moçotéguy, P., Candusso, D., & Hissel, D. (2009). A review on polymer electrolyte membrane fuel cell catalyst degradation and starvation issues: Causes, consequences and diagnostic for mitigation. Journal of Power Sources, 194(1), 130-145.

[72] Li, Z., Outbib, R., Giurgea, S., Hissel, D., Giraud, A., & Couderc, P. (2018). Fault diagnosis for fuel cell systems: A data-driven approach using high-precise voltage sensors. Renewable Energy.

[73] Steiner, N. Y., Hissel, D., Moçotéguy, P., & Candusso, D. (2011). Diagnosis of polymer electrolyte fuel cells failure modes (flooding & drying out) by neural networks modeling. International Journal of Hydrogen Energy, 36(4), 3067-3075.

[74] Baschuk, J. J., & Li, X. (2001). Carbon monoxide poisoning of proton exchange membrane fuel cells. International Journal of Energy Research, 25(8), 695-713.

[75] Petrone, R., Zheng, Z., Hissel, D., Péra, M. C., Pianese, C., Sorrentino, M., ... & Yousfi-Steiner, N. (2013). A review on model-based diagnosis methodologies for PEMFCs. International Journal of Hydrogen Energy, 38(17), 7077-7091.

[76] Zheng, Z., Petrone, R., Péra, M. C., Hissel, D., Becherif, M., Pianese, C., ... & Sorrentino, M. (2013). A review on non-model based diagnosis methodologies for PEM fuel cell stacks and systems. International Journal of Hydrogen Energy, 38(21), 8914-8926.

[77] Isermann, R. (1997). Supervision, fault-detection and fault-diagnosis methods—an introduction. Control engineering practice, 5(5), 639-652.

[78] Becherif, M., Hissel, D., Gaagat, S., & Wack, M. (2010). Three order state space modeling of proton exchange membrane fuel cell with energy function definition. Journal of Power Sources, 195(19), 6645-6651.

[79] Jemeı, S., Hissel, D., Péra, M. C., & Kauffmann, J. M. (2003). On-board fuel cell power supply modeling on the basis of neural network methodology. Journal of Power Sources, 124(2), 479-486.

[80] Fouquet, N., Doulet, C., Nouillant, C., Dauphin-Tanguy, G., & Ould-Bouamama, B. (2006). Model based PEM fuel cell state-of-health monitoring via ac impedance measurements. Journal of Power Sources, 159(2), 905-913.

[81] Kim, J., Lee, I., Tak, Y., & Cho, B. H. (2012). State-of-health diagnosis based on hamming neural network using output voltage pattern recognition for a PEM fuel cell. International journal of hydrogen energy, 37(5), 4280-4289.

[82] Hissel, D., Candusso, D., & Harel, F. (2007). Fuzzy-clustering durability diagnosis of polymer electrolyte fuel cells dedicated to transportation applications. IEEE Transactions on Vehicular Technology, 56(5), 2414-2420.

[83] Jang, J. S. (1993). ANFIS: adaptive-network-based fuzzy inference system. IEEE transactions on systems, man, and cybernetics, 23(3), 665-685.

[84] Escobet, T., Feroldi, D., De Lira, S., Puig, V., Quevedo, J., Riera, J., & Serra, M. (2009). Model-based fault diagnosis in PEM fuel cell systems. Journal of Power Sources, 192(1), 216-223.

[85] Isermann, R. (2006). Fault-diagnosis systems: an introduction from fault detection to fault tolerance. Springer Science & Business Media.

[86] Niya, S. M. R., & Hoorfar, M. (2013). Study of proton exchange membrane fuel cells using electrochemical impedance spectroscopy technique–A review. Journal of Power Sources, 240, 281-293.

[87] Jespersen, J. L., Schaltz, E., & Kær, S. K. (2009). Electrochemical characterization of a polybenzimidazole-based high temperature proton exchange membrane unit cell. Journal of Power Sources, 191(2), 289-296.

[88] Wu, J., Yuan, X. Z., Wang, H., Blanco, M., Martin, J. J., & Zhang, J. (2008). Diagnostic tools in PEM fuel cell research: Part I Electrochemical techniques. International journal of hydrogen energy, 33(6), 1735-1746.

[89] Mainka, J., Maranzana, G., Dillet, J., Didierjean, S., & Lottin, O. (2014). On the estimation of high frequency parameters of proton exchange membrane fuel cells via electrochemical impedance spectroscopy. Journal of Power Sources, 253, 381-391.

[90] Kim, J., Lee, I., Tak, Y., & Cho, B. H. (2013). Impedance-based diagnosis of polymer electrolyte membrane fuel cell failures associated with a low frequency ripple current. Renewable energy, 51, 302-309.

[91] Li, H., Zhang, S., Qian, W., Yu, Y., Yuan, X. Z., Wang, H., ... & Cheng, T. T. (2012). Impacts of operating conditions on the effects of chloride contamination on PEM fuel cell performance and durability. Journal of Power Sources, 218, 375-382.

[92] Wang, Y., Liu, G., Wang, M., Liu, G., Li, J., & Wang, X. (2013). Study on stability of self-breathing DFMC with EIS method and three-electrode system. International journal of hydrogen energy, 38(21), 9000-9007.

[93] Morin, A., Peng, Z., Jestin, J., Detrez, M., & Gebel, G. (2013). Water management in proton exchange membrane fuel cell at sub-zero temperatures: An in operando SANS-EIS coupled study. Solid State Ionics, 252, 56-61.

[94] Travassos, M. A., Lopes, V. V., Silva, R. A., Novais, A. Q., & Rangel, C. M. (2013). Assessing cell polarity reversal degradation phenomena in PEM fuel cells by electrochemical impedance spectroscopy. International Journal of Hydrogen Energy, 38(18), 7684-7696.

[95] Reshetenko, T. V., Bethune, K., Rubio, M. A., & Rocheleau, R. (2014). Study of low concentration CO poisoning of Pt anode in a proton exchange membrane fuel cell using spatial electrochemical impedance spectroscopy. Journal of Power Sources, 269, 344-362.

[96] Jeppesen, C., Polverino, P., Andreasen, S. J., Araya, S. S., Sahlin, S. L., Pianese, C., & Kær, S. K. (2017). Impedance characterization of high temperature proton exchange membrane fuel cell stack under the influence of carbon monoxide and methanol vapor. International Journal of Hydrogen Energy, 42(34), 21901-21912.

[97] Zhiani, M., & Majidi, S. (2013). Effect of MEA conditioning on PEMFC performance and EIS response under steady state condition. International journal of hydrogen energy, 38(23), 9819-9825.

[98] Baricci, A., Mereu, R., Messaggi, M., Zago, M., Inzoli, F., & Casalegno, A. (2017). Application of computational fluid dynamics to the analysis of geometrical features in PEM fuel cells flow fields with the aid of impedance spectroscopy. Applied Energy, 205, 670-682.

[99] Hong, P., Xu, L., Jiang, H., Li, J., & Ouyang, M. (2017). A new approach to online AC impedance measurement at high frequency of PEM fuel cell stack. International Journal of Hydrogen Energy, 42(30), 19156-19169.

[100] Hinaje, M., Sadli, I., Martin, J. P., Thounthong, P., Raël, S., & Davat, B. (2009). Online humidification diagnosis of a PEMFC using a static DC–DC converter. International journal of hydrogen energy, 34(6), 2718-2723.

[101] Narjiss, A., Depernet, D., Candusso, D., Gustin, F., & Hissel, D. (2008). On-line diagnosis of a PEM Fuel Cell through the PWM converter. Proceedings of FDFC 2008.

[102] Doan, V. T., Vu, V. B., Vu, H. N., Tran, D. H., & Choi, W. (2015, June). Intelligent charger with online battery diagnosis function. In Power Electronics and ECCE Asia (ICPE-ECCE Asia), 2015 9th International Conference on (pp. 1644-1649). IEEE.

[103] Bethoux, O., Hilairet, M., & Azib, T. (2009, November). A new on-line state-of-health monitoring technique dedicated to PEM fuel cell. In Industrial Electronics, 2009. IECON'09. 35th Annual Conference of IEEE (pp. 2745-2750). IEEE.

[104] Hong, P., Li, J., Xu, L., Ouyang, M., & Fang, C. (2016). Modeling and simulation of parallel DC/DC converters for online AC impedance estimation of PEM fuel cell stack. International Journal of Hydrogen Energy, 41(4), 3004-3014.

[105] Varnosfaderani, M. A., & Strickland, D. (2016, September). Online impedance spectroscopy estimation of a battery. In Power Electronics and Applications (EPE'16 ECCE Europe), 2016 18th European Conference on (pp. 1-10). IEEE.

[106] Katayama, N., & Kogoshi, S. (2015). Real-time electrochemical impedance diagnosis for fuel cells using a DC–DC converter. IEEE Transactions on Energy Conversion, 30(2), 707-713.

[107] Depernet, D., Ba, O., & Berthon, A. (2012). Online impedance spectroscopy of lead acid batteries for storage management of a standalone power plant. Journal of Power Sources, 219, 65-74.

[108]